

Combustion dynamics of polymer wastes in a bubbling fluidized bed

Witold Żukowski ^{a,*}, Dawid Jankowski ^a, Jerzy Baron ^a, Jan Wrona ^b

^a Faculty of Chemical Engineering and Technology, Cracow University of Technology, ul. Warszawska 24, 31-155, Cracow, Poland

^b Faculty of Environmental and Power Engineering, Cracow University of Technology, ul. Warszawska 24, Cracow, 31-155, Poland



ARTICLE INFO

Handling editor: Cecilia Maria Villas Bóas de Almeida

Keywords:
Combustion
Fluidized bed
Polymers
Biomass

ABSTRACT

This paper compares the combustion of selected artificial polymers and biomasses in a fluidized bed reactor. Two types of the artificial polymers were tested. The first one was used in packaging: polyethylene, polypropylene, polyethylene terephthalate, and polystyrene. The second one included construction polymers: polyamide, polycarbonate, copolymer acrylonitrile-butadiene-styrene and polyvinyl chloride. For comparison the combustion of the biomasses in the form of processed briquettes and pellets as well as beech and pine wood samples was also presented. The tests were carried out in a bubble fluidized bed built of quartz sand (granulation 0.385–0.43 mm). In the first part of the research, the samples of polymers and biomasses were burned in the presence of gaseous fuel at a bed temperature of approximately 850°C. In the second part, after heating the bed to a temperature of approximately 900°C, the supply of gaseous fuel was closed. The samples were dosed when the bed was fluidized only with air. It has been found that the combustion times for packaging and construction materials (samples: 0.1–1.8 g) were similar ($T = 10.8$ s), except for the polyvinyl chloride and polyamide samples whose combustion time was twice as long. The time of combustion of the biomass particles depended strongly on the sample mass rather than its type, which was of less importance. The presence of radicals resulting from liquefied petroleum gas combustion influenced the process of carbon chain fragmentation, thus shortening the time of combustion of polymers in comparison to the tests carried out without a gaseous supporting fuel. The combustion of polymers and biomasses was accompanied by the release of pyrolytic gases which, after mixing with oxidiser, ignited in regular time intervals, with frequencies 2 and 1.1 Hz. The general scheme of sequence of events making up the dynamics of the process was presented.

1. Introduction

Modern civilization has developed based on fossil fuels, which in 2018 still covered about $\frac{1}{4}$ of the global electricity demand (IEA, 2018). The global electricity demand was approx. 26,615 TWh in 2018 (Ortiz et al., 2020). The EU policy, to counteract climate change, assumes reaching that by 2030 the share of renewable energy will increase to 32% (European Parliament, 2018a). The policy is designed to reduce greenhouse gas emissions by 40% compared to 1990 also (European Parliament, 2018b). All these activities show global trends of the energy sector, which consist in decreasing the share of fossil fuels. (Chen et al., 2021). The use of renewable sources of energy leading to the decarbonisation should be the driving force behind further economic growth. If we take into account the estimated energy demand of approx. 42,500 TWh in 2040 (Ortiz et al., 2020) and the increase of the population to the level of 10 billion in 2060 (Papadis and Tsatsaronis, 2020), there are questions whether a complete energy transformation is possible and in

what period of time. Regardless of the answers to these questions, changes in the energy sector will not take place suddenly, and the energy deficit will continue to be met by conventional fuels (IEA, 2017). In the transition period, materials such as biomasses (Nordin et al., 2020) and alternative fuels (Kaewbudddee et al., 2020) may play an important role. In the case of the latter, if they are obtained from waste, it will additionally contribute to reducing the stream of waste sent to the landfills. It is forecasted that the amount of waste generated in 2050 will reach 3.4 billion tonnes per year (Wienczel et al., 2020).

Polymers produced today are considered to be highly environmentally harmful materials. However, it is possible to significantly reduce the amount of wastes, e.g. by ecologically oriented selections of plastics, their reduction or by designing devices with the highest possible degree of recycling and development of new technologies enabling energy recovery from waste (Baytekin et al., 2013).

Mechanical recycling, energy recovery and raw material recycling are options for the management of used polymers. Mechanical recycling involves sorting and shredding of used polymers without changing their

* Corresponding author.

E-mail address: witold.zukowski@pk.edu.pl (W. Żukowski).

Nomenclature	
<i>Symbols</i>	
ABS	acrylonitrile butadiene styrene
BFB	bubbling fluidized bed
CFB	circulating fluidized bed
CLA	chemiluminescence method
df	degrees of freedom
EC	electrochemical method
FID	flame ionization detector
FTIR	Fourier-transform infrared spectroscopy
HDPE	high density polyethylene
k	number of time points (moving average)
LDPE	low density polyethylene
LPG	liquefied petroleum gas
m	mass, g
MPW	municipal plastic waste
MSW	municipal solid waste
MSE	mean squared error
NDIR	nondispersive infrared method
p	probability of testing
PA	polyamide
PC	polycarbonate
PET	polyethylene terephthalate
PP	polypropylene
PS	polystyrene
PVC	polyvinyl chloride
R ²	coefficient of determination
SEE	Standard Error of the Estimate
SD	standard deviation
T	average combustion time for packaging materials, s
t	the value of Student test
t _{i,j}	the critical value of Student test
Tign	ignition temperature, °C
T _{mel}	melting temperature, °C
W	heating value, MJ kg ⁻¹
VOC	volatile organic compounds
̄V _{ex}	stream of exhaust gases, kmol s ⁻¹
̄Q	stream of heat, W
<i>Greek symbols</i>	
λ	thermal conductivity coefficient, W m ⁻¹ K ⁻¹

chemical structure. Its purpose is to obtain a regranulate suitable for reuse. This type of recycling is used for homogeneous and clean materials. The raw material recycling includes e.g. the reuse of processed waste, multiple use of products for the same purposes and chemical recycling. An energy recovery from polymers can be realized e.g. by co-combustion together with municipal waste in waste incineration plants due to their high calorific value (Costiuc et al., 2015). This method is recommended in the case of mixed and contaminated fractions of these wastes, and the results are electricity and/or thermal energy.

Although the combustion of polymers is much more common, other technologies related to raw material recycling, i.e. thermolysis and chemolysis, should not be forgotten. In the thermolysis process, which most often uses high-temperature processes such as pyrolysis (Zhang et al., 2021), gasification or hydrogenation, the main products are liquids, char and light hydrocarbons. In the case of the chemolysis process we obtain monomers that can be used in the production of new polymers. Therefore, that technologies allow virtually full recycling of the raw material, which is becoming more and more important due to the growing concerns about the environment (Wrona, 2014). One of the examples of polymers that can be successfully used in the thermolysis process to produce high-value ingredients for the production of diesel oil, gasolines and heating oils are polyolefins. However, thermolysis is a complicated process carried out most often in the presence of catalysts that are not only, but also not necessarily economical (Scheirs and Kaminsky, 2006).

Polymers that cannot be reused must be stocked. We can distinguish two groups here: non-degradable and biodegradable. In Europe about 24.9% of the polymer waste collected in 2019 was landfilled. This is still a large amount, that should be reduced if possible or non-biodegradable polymers should be replaced with biodegradable polymers (Marczak et al., 2020).

In 2019, the global production of polymers reached almost 370 million tons (in Europe about 58 million tons). The distribution of polymer demand (EU28 + NO/CH) by sector in 2019 shows that the packaging industry, construction, and the automotive industry are the largest end-user markets. The most commonly used polymers in European countries include PE, PP, PVC, PET and PUR. Currently, around 30 million tonnes of polymer waste is collected in the EU28 + NO/CH in order to further its treatment. This accounts for slightly more than half of their production in Europe, which shows the scale of the problem to be

solved in the future (PlasticsEurope, 2020).

In Europe the most used method of polymer waste management is energy recovery (42.6% in 2019) by combustion them in specialized installations, e.g. waste incineration plants. Direct combustion of polymers leads to a reduction in the volume of waste by more than 90%, which is beneficial for its disposal in landfills (PlasticsEurope, 2020). There are still environmental problems that don't differ from those associated with the combustion of other waste: emissions of CO₂, NO_x, SO_x, as well as the generation of volatile organic compounds, smoke (solid particles) and heavy metals associated with the dust (Ergut et al., 2007). In addition, the combustion of polymers such as polyvinyl chloride (PVC), polyethylene (PE), polystyrene (PS) and polyethylene terephthalate (PET) produces carcinogens such as polycyclic aromatic hydrocarbons and dioxins (Westblad et al., 2002).

2. Background

2.1. The importance of additives in the thermal decomposition of polymer waste

Municipal waste, which with an average calorific value of 10 MJ kg⁻¹ can be incinerated as mixed (Zaini et al., 2020). Mixed polymers are the most calorific fraction MSW (approx. 35 MJ kg⁻¹) (Mazzoni and Janajreh, 2017). The average calorific value of biomass from MSW in Europe is approx. 14 MJ kg⁻¹ (Zhou and Wang, 2017).

Mixed polymers are characterised by considerable heterogeneity with respect to their composition as well as physical and chemical properties. This may lead to difficulties in conducting and describing the process of their thermal decomposition (Al-Salem, 2017). Polymer construction materials contain additives which decrease their combustibility. These additives may, among others, lower temperature in the combustion zone, create a film on the surface of the burning solid which impedes oxygen access to the reaction zone, or create radicals inhibiting the combustion. Combustion inhibitors in gaseous products react with free radicals and cause their substitution with less active ones (Roberts, 2017). As a result, the temperature of the flame decreases and the thermal decomposition is slowed down. The presence of flame retardants in the combusted material promotes the emission of toxic components, e.g. dioxins and furans (Yasin et al., 2017). Polymers' combustion with the presence of flame retardants takes place according

to several simultaneous mechanisms, but there is a dominating mechanism which changes in time (Hayhurst, 2013). The proposed kinetic models refer mainly to one type of polymer (Ranzi et al., 1997) or their two- or three-component compounds (Faravelli et al., 2003). While analysing the pyrolysis of the polymer compounds Williams and Williams (1999) demonstrated that HDPE, LDPE and PP decomposed into aliphatic compounds consisting of alkanes, alkenes and alkadienes. The oils extracted from PVC were dominated by aromatic ingredients, and the products of PS and PET decomposition containing aromatic groups also decomposed into hydrocarbons with higher levels of aromatic ingredients. Williams and Williams (1999) also stated that the average particle mass of the wax obtained from mixed polymers was smaller than expected with respect to oils/waxes obtained from the decomposition of single, unmixed polymers. The MPW fraction is not only a valuable energy resource, but also a rich source of hydrocarbons that can be recycled to the chemical industry (Berkowicz et al., 2020). In the conditions of real-world waste disposal, the MPW consists of various polymers, which are frequently contaminated with organic waste. In addition, modern polymer materials may contain unusual functional additives, like a poultry waste (McGauran et al., 2021), cork (La Rosa et al., 2014) or flax (Gomez-Campos et al., 2021). Their aims are, among others, to reduce the consumption of raw materials in the production of polymer materials and to reducing their weight, while maintaining the desired mechanical and physicochemical properties. These additives can significantly differ in the mechanism and kinetics of combustion in comparison to clean polymers, which, when combined, creates additional difficulties in the description of this process (Gomez-Campos et al., 2021).

In the management of polymer waste, in addition to the recovery of the material itself, which can be reused, their valorization plays an important role (Dwivedi et al., 2019). Fuels, e.g. oil, can be produced from polymer waste (Kasara et al., 2020). Polymer thermoplastic waste is used for valorization and metallic ore mining tailing from which lightweight aggregates are produced (Moreno-Maroto et al., 2019). From polymer waste and empty cotton boll, Bio-oil gasoline and Biochar is made (Patel et al., 2021). Flame retardants used in the production of polymers can be a problem. Yasin et al. (2017) removed flame retardants from cotton fabric using the Fenton reaction. TGA analysis indicated a similar temperature of material decomposition as for the sample containing FR. Similar functional groups were identified in both fabrics using FTIR. The calorific value (HHV) also did not change after the degradation of the FR in the sample. The synthesis gas obtained by gasification in a fountain bed of fabrics containing and without FR had a similar composition (Yasin et al., 2020).

2.2. Influence of temperature and presence of catalyst on thermal decomposition of polymer waste

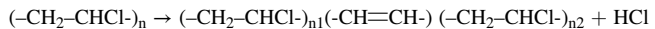
The rising temperature of polymer material initiates a sequence of phase transitions and chemical reactions (Boryniec and Przygocki, 2000). The mechanism of polymers' combustion depends on the temperature range (Burgess et al., 2011). As a result of heat, polyolefins melt with a sudden emission of gaseous hydrocarbons. These materials constitute 80% of the manufactured polymers and are characterised by a relatively simple structure in comparison to construction polymers. During their thermal decomposition C–C bonds break in different parts of the chain resulting in the creation of low molecular weight hydrocarbons and small amounts of monomers (Berkowicz et al., 2020). The use of a catalyst (Fe_2O_3) during the combustion of polyolefins increases the degree of their conversion to CO_2 (an increase of about 24%), which is already achieved at a temperature of 500°C in a fluidized bed (Żukowski and Berkowicz, 2019). The ramification of the chain leads to decreasing the thermostability of the polymer. In the case of construction materials (e.g. PVC), the first phase of thermal decomposition causes abstraction of the side groups from the carbon chain, which can subsequently react with each other or take part in a cyclisation reaction

with another particle in the gaseous phase.

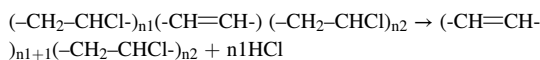
The remainder of the chain creates a layer of char (similar to biomass combustion), which increases the diffusion resistance and leads to extinguishing the flame (Chern and Hayhurst, 2010). Sometimes the remaining char can have greater calorific value than polymer (PVC) and undergoes further thermal decomposition. The rate of pyrolysis of the polymer is controlled by the outside warmth getting into the particle. For this reason, the conditions in which the process occurs are of vital importance. Burgess et al. (2011) have indicated that above 640°C the combustion time of HDPE is influenced mostly by the rate of the combustible gases diffusion from polymer aggregate and sand, and with an inconsiderable impact of the bed temperature. The time of polymer combustion in a fluidized bed relies on the mass of the particle (Burgess et al., 2011) and its initial dimensions. In the initial stage of solid fuel combustion, the speed of decomposition is determined by the heat transfer to the particle. Polymers are good insulators ($\lambda \sim 0.12 \text{ W m}^{-1}\text{K}^{-1}$), which does not contribute to a fast growth of temperature of the combusted particle. The increase of the particle's diameter is accompanied by the growth of the Biot number value. Consequently, the combustion times of a singular polymer sample were longer than that of several samples of the same mass but with smaller initial diameters (Baron et al., 2006). Furthermore, Menon et al. (2017) have observed that while combusting parafin and glycerine in the fluidized bed, similar processes occurred. Both materials behaved like polymers in a heated bed that is, they produced diffusion flames above its surface and caused exploding bubbles after mixing with the air inside the bed. On the other hand, in the temperature of 900°C, the times of singular particles combustion were noticeably shorter than the ones applied simultaneously. In both situations the samples' combustion time was proportional to the square of their diameter.

2.3. Characteristic stages of thermal decomposition of PVC waste

Thermal decomposition of PVC is initiated in the temperature of 227–277°C which is considerably lower in comparison to the decomposition conditions for PE, PP, PET, PS. It is caused by the presence of thermally unstable structures and polymer chains defects (Yu et al., 2016). Thermal elimination of HCl is triggered by the reaction:



Reactive chlorine atoms in an allyl position arising from the initiation reaction are responsible for the acceleration of the abstraction of subsequent HCl particles from the polymer chain (German, 2009). C1-radicals created during the decomposition reaction with H- and OH-radicals leading to the retardation of the polymer combustion. The energy of the C–C1 bond is inferior to the energies of C–C and C–H bonds and therefore, it is the C–C1 bond which is the first to undergo the process of thermal dissociation (Sun et al., 2007). The loss of HCl in a PVC particle leads to the creation of conjugate double bonds in the polymer chain:



In the next cycle, the allyl group with two double bonds and then with three double bonds, and so forth, is created (German, 2009).

According to Lopez et al. (2011) during the first stage of thermal decomposition the PVC loses about 65% of its mass. In this part of the process, in a relatively low temperature, the PVC particle releases a greater amount of chlorine. Within the range of 280–320°C polymer loses about 95.5%_{mas} of the initial mass of chlorine (Yuan et al., 2014). As stated by Sun et al. (2007), the low temperature of the PVC dechlorination process is caused by a free radical chain reaction which requires less activation energy for its initiation. The mechanism of the PVC thermal dehydrochlorination is not fully known – with this respect three mechanisms are considered: radical, ion and an agreed mechanism

(German, 2009). Sanchez-Jimenez et al. (2010) claim that dechlorination may occur in accordance with two different kinetic models for two separate chlorine groups. In a lower temperature it happens on the basis of an embryo growth model and in a higher temperature the process controls the speed of chlorine diffusion. During the second stage of pyrolysis radical reactions accelerate together with the temperature growth (350–525°C) and the cyclisation reactions lead to the creation of aromatic hydrocarbons (Yu et al., 2016). What follows is the random breaking of the carbon chain and recombination reactions (Jordan et al., 2001). On the one hand, HCl accelerates the process of pyrolysis and acts as a catalyst, and on the other, it dilutes a combustible mixture and reacts with its ingredients (Starnes and Ge, 2004). The HCl activity and autocatalytic reaction cause a sudden acceleration of PVC decomposition after a short initiation stage (Patel et al., 1992). There is then an observed retarding after achieving a sample decomposition at the level of 0.7 (Troitskii and Troitskaya, 1999). It is difficult to confirm the activity of HCl unanimously when it is not clear whether the particle comes from an elimination reaction or a chain propagation (Troitskii and Troitskaya, 1995). Intermolecular reactions lead to the networking of the non-volatile products and the surface of PVC is covered with a protective layer of char which stops oxygen diffusion and heat transfer inside the sample and consequently retards the process of decomposition. Saeed et al. (2004) stated that the residue matter remaining after the pyrolysis of PVC in BFB within the temperature range between 200 and 400°C contained less than 0.1%_{mas} of chlorine, 93.6%_{mas} of carbon and approximately 6.3%_{mas} of hydrogen. There was a congenial coke composition during the process of combustion of PVC in CFB in the temperature of approximately 800°C. The layer of char on the surface of polymer together with the application of combustion retardants is one of the methods used in reducing combustibility of polymers (Pike et al., 1997). The flame retardants, which catalyse the formation of the char layer constitute an alternative to halogen compounds – they are characterised by small emission of smoke and toxic gases (Grand and Wilkie, 2000).

2.4. Structure and thermal decomposition of biomass

Biomass consists of three major ingredients: cellulose (40–50%), hemicellulose (20–40%) and lignin (15–30%) whose content depends on the type of the biomass (Williams and Williams, 1999). While heating the sample the hemicellulose is the first to decompose (180–350°C), then the lignin which decomposes in the temperature of 250–500°C. The last is cellulose with a decomposition temperature of 275–350°C (Boryniec and Przygocki, 1999). The structure of the cellulose is extremely important in the process of thermal decomposition. In the crystalline state of cellulose its energy to activate the decomposition reaction is 140–170 kJ mol⁻¹ and in the amorphous state it is 54 kJ mol⁻¹. The initial stage of the biomass pyrolysis is characterised by the reaction of dehydration and netting. Above 300°C weak C–O–C and C–C bonds in the glycoside link become disrupted and tiny unstable radicals are created. Their quick recombination leads to the emission of CO, CO₂, low molecular weight, volatile hydrocarbons, and water. Moreover, it causes the formation of a charred structure on the surface of the particle. Both, disruption of side groups and cracking of the C–O bonds result in depolymerisation of cellulose. Before the particle surface is charred, part of the volatile gaseous products is suddenly released (Chern and Hayhurst, 2012). A porous and charred surface of the biomass acts as an insulator which restricts heat and mass conversion with the surrounding environment and constitutes a protective layer of the combusted biomass particle (Chern and Hayhurst, 2010). The same properties of the char limit the combustibility of the construction polymers (Singh and Ruj, 2016).

2.5. The use of fluidized bed in the combustion process

In order to ensure favourable conditions for heat and mass transfer,

the process of MPW combustion should be carried out with the application of a fluidized bed. In addition to the fluidized bed technology, grate boilers are often used to incinerate waste (Dong et al., 2018). Waste can also be incinerated, among others in rotary kilns (Kosajan et al., 2020). Over the last few years the fluidized technology has found a number of applications in the process of combustion of alternative fuels and wastes. Such fuel can be palm oil (Razuan et al., 2011), mushroom compost (Finney et al., 2009) or vinasse (a by-product of the sugar industry) (Akram et al., 2015). The use of a catalyst as a bed material enables better conversion of fuels to CO₂, lower NO_x emissions and a lower combustion temperature. The catalytic bed (iron-chromium catalyst) also creates the right conditions also for the production of *fuel of the future*, which is hydrogen from biomethanol (Żukowski and Berkowicz, 2017) or raw material synthesis for the polymers industry e.g. 2, 6-dimethylphenol (26DMP) from o-cresol (Berkowicz et al., 2013). Promising results are obtained when cenospheres are used as a bed material, the density of which (<1 g cm⁻³) is lower than that of sand (~2.6 g cm⁻³). As a result, the bed material more easily transforms into a fluidized state, and the dipped polymer particle floats in its entire volume (Żukowski and Berkowicz, 2019). The fluidized bed made of cenospheres also provides an appropriate combustion environment for liquid fuels (glycerol, paraffin oil) and low-density solid fuels (paraffin wax) (Żukowski and Berkowicz, 2019). As a result of intensive mixing of the bed, it is possible to collect gaseous products from the sample's environment and to maintain a constant concentration of oxidiser in the bed. When the temperature gradient in the bed is inconsiderable, the speed of a polymers combustion is determined by the temperature of the process, the type and size of the polymer and additives applied in polymers.

2.6. Purpose and scope of research

Combustion of organic substances, including polymers, may proceed with different dynamics and lead to the formation of flue gases of a different composition. The course of the process over time, and total time of conversion depend on the process conditions and the reaction environment in which the process is organized. The environment of a fluidized bed reactor with a bubble fluidized bed has favourable process parameters, particularly when it comes to organizing rapid combustion processes. However, the combustion process itself is different depending on the fuel used. The aim of the work is to indicate the unique phenomena that occur during the combustion of polymers, which shape the dynamics of the process and which should be taken into account when using this process for the thermal transformation of polymers, regardless of the scale of the device used. Due to proper consideration of, inter alia, the reaction time of the materials, an effective total fuel conversion can be obtained, hence the appropriate quality of the final (gaseous) products of the process. This means that the combustion process must be organized according to the so-called 3T rule (Scharler et al., 2020). There must be an adequate combustion Time, Turbulence and Temperature. These conditions can be provided by the use of a fluidized bed reactor. Therefore, examining the combustion dynamics of the selected type of waste seems to be of key importance for the proper planning, e.g. of the residence time of fuel particles in the entire volume of the fluidized bed (Liu et al., 2021). The article discusses the problem of managing the growing amount of polymer waste and presents a practical way to recover the energy deposited therein. The incineration of waste significantly contributes to the reduction of their stream going to landfills (Malav et al., 2020).

3. Experimental setup

The experiments were carried out in a laboratory installation/plant. A fluidized reactor together with control and a measurement apparatus (Fig. 1) were frequently utilised in research on the combustion of coal, liquid gas fuels and all types of waste.

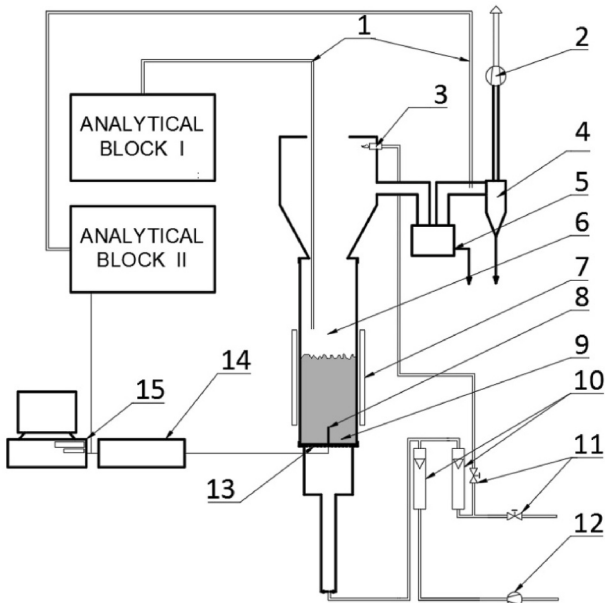


Fig. 1. Diagram of research installation, 1-heated probe/tube for sampling exhaust gases, 2-exhaust fan, 3-outlet burner, 4-cyclone, 5-settling chamber, 6-freeboard, 7-movable thermal shield, 8-thermocouple, 9-fluidized bed, 10-rotametres, 11-fuel feeding valves, 12-air blower, 13-distributor, 14-A/D converter for signal from thermocouples, 15-computer recording the results.

Laboratory fluidized reactor with the power of about 10 kW comprises of a quartz tube whose internal diameter is 98 mm and its height is 500 mm. This tube rests on a steel gas distributor which is 1 mm thick. The perforated part of the distributor is covered with equally spaced 0.6 mm holes whose total area is 1.6% of the whole distributor. $0.033 \pm 0.01 \text{ L s}^{-1}$ of gas fuel (LPG) was introduced into the distributor after being mixed with the air stream which was $1.66 \pm 0.03 \text{ L s}^{-1}$. The combustion of LPG mixed with air took place with the excess air coefficient λ of 1.8. Schematic diagram of a fluidized bed reactor shown in Fig. 2.

Samples of exhaust gases were collected in two places and then distributed to the analysers in the temperature of 130°C . For the first analytical block the samples were collected in the zone above the bed at the distance of 495 mm from the bottom of the sieve, whereas for the second block they were collected from behind the settling chamber. In the first analytical block the contents with measure tolerance of $\text{O}_2 \pm 0.1\%$, $\text{CO} \pm 16 \text{ ppm}$, $\text{NO} \pm 8 \text{ ppm}$, $\text{NO}_2 \pm 1 \text{ ppm}$, $\text{SO}_2 \pm 16 \text{ ppm}$ in the exhaust was determined by means of the EC method by ECOM SG Plus analyser. The NDIR method was applied in specifying the content of $\text{CO} \pm 2 \text{ ppm}$, $\text{CO}_2 \pm 0.2\%$ and $\text{SO}_2 \pm 2 \text{ ppm}$. The content of $\text{NO}_x \pm 5 \text{ ppm}$, was analysed with the CLA method. Both methods were carried out using a PG-250 analyser (Horiba co.). The content of $\text{VOC} \pm 20 \text{ ppm}$ with FID method by 3-200 analyser (JUM Engenering GmbH). In the second analytical block, $\text{O}_2 \pm 0.2\%$, $\text{CO} \pm 10 \text{ ppm}$, $\text{NO} \pm 5 \text{ ppm}$, $\text{NO}_2 \pm 5 \text{ ppm}$, $\text{SO}_2 \pm 10 \text{ ppm}$ were analysed using the EC method by VARIO PLUS analyser (MRU GmbH). Further organic and inorganic compounds were marked by means of the FTIR method using DX-4000 (Gasmet).

The process of samples combustion was recorded with a camera, whose lens was placed at the level of the bed at a distance of 2.5 m from the reactor's axis. Depending on the character of the experiments, the picture could be recorded continuously or periodically with the frequency of 500 frames per second and the maximum resolution of 2046×1086 pixels. Based on these recordings, the combustion time could be determined with an accuracy of 0.002 s. Using mathematical notation, each of the three layers of the colour picture (R, G, B) constitutes a matrix whose number of rows and columns corresponds to the camera's resolution. A single pixel is thus described by three numbers (3×8 bits)

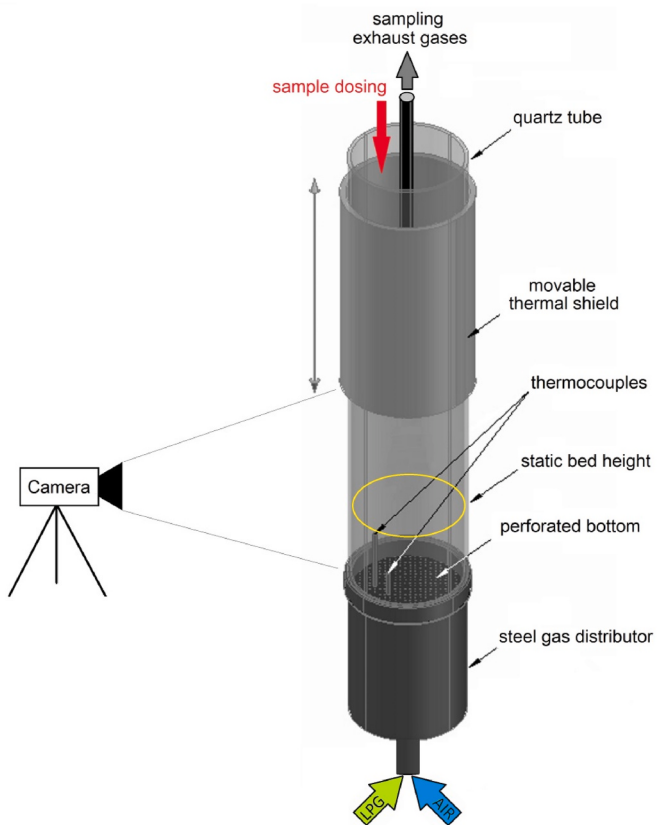


Fig. 2. Schematic diagram of research reactor.

indicating brightness of the object in three transmission bands of colour RGB filters. The brightness of the black pixel is equal to 0. The analysis of combustion dynamics was based on the data collected from the red colour matrix, by averaging the values of brightness of all pixels to one number. A detailed description of methodology used in transforming a colour picture into a one number notation for each pixel was provided in paper (Zukowski et al., 2009).

A small gradient in the temperature of the bed enabled the application of two thermocouples located 20 and 50 mm above the distributor. The analog signal from the thermocouples of 1 Hz frequency was directed to the A/D converter where it was amplified and transformed into a digital signal which was saved in memory. The recorded data was used to calculate the average temperature of the bed with 1°C tolerance.

The analysis of the dynamics of the tested samples decomposition was based on the alterations in the concentration of CO_2 in exhaust fumes and the average temperature of the bed. When possible, the digital record of the combustion was also used.

The CHN analysis of the test samples was performed using 2400 C/H/N analyser (PerkinElmer).

3.1. Tested materials

The paper presents the dynamics of combustion for 12 polymeric materials, 8 types of polymers and 4 types of biomasses. The classification of polymers relies on their applicability. They are divided into packaging polymers such as, LDPE, HDPE, PP, PS, PET and construction polymers like: PA, ABS, PC and PVC. All of them are parts of municipal waste and they differ in ignition temperature (T_{ign}), melting temperature (T_{melt}), density (Mark, 2007) and heating value (W) (Table 1) (Walters et al., 2000). Basic analysis of the samples indicates that the polycarbonate utilised in the tests was obtained from bisphenol A and phosgene. There are 31.6% of incombustible parts in the polyamide. The

Table 1
Properties of polymer materials.

Sample	T _{ign} , °C	T _{melt} , °C	ρ, g cm ⁻³	W, MJ kg ⁻¹
Packaging				
LDPE	349	107–124	0.925	44.6
HDPE		122–137	0.950	
PP	570	158–168	0.910	42.7
PET	355	255–264	1.345	23.2
PS	488–496	100–120	1.045	42.0
Construction				
PA	460	222	1.130	33.0
PC	580	140–150	1.200	30.3
ABS	416	88–125	1.045	38.1
PVC	435–557	75–110	1.400	18.0
Solid wood				
Pine	365	–	0.545	14.3
Beech	460	–	0.725	14.6
Processed biomass				
Pellets	310–350	–	1.12	18.0
Briquettes		–	1.2	18.5

samples of biomass constituted solid fragments of pine and beech wood as well as briquettes and pellets processed from sawdust and forest waste (Table 1) (Horvath and Balog, 2013).

3.2. Research methods

The samples were combusted periodically with the addition of LPG gas and in a pre-heated bed without LPG. During the first stage of the test, the bed was heated to $850 \pm 1^\circ\text{C}$ and after obtaining a constant concentration of CO, CO₂, and VOC in exhaust gases, with permanent gas fuel inflow, the tested materials were supplied periodically. The interval between subsequent applications of samples in the bed was specified by the rate in which the process parameters would return to the original state. In the second stage, after heating the bed to $900 \pm 1^\circ\text{C}$ the gas supply was closed, and a single sample was applied.

4. Results and discussion

4.1. Behaviour of polymers and biomass in heated fluidized bed

Thermoplastic polymeric materials incinerate in a specific manner. Under the influence of heat they soften, liquify and ultimately undergo pyrolysis mainly to low mass particle volatile organic compounds, which are subsequently mixed with air and combusted (Baron et al., 2006).

Polymer materials brought into the heated bed, just like paraffin, melted and became viscous (Menon et al., 2017). Together with the quartz sand they formed aggregates and increased their density. Such a particle, whose initial density was smaller than the density of the bed, combined with sand, increased its mass, and circulated in the whole volume of the bed (Baron et al., 2006).

In the first series of tests, the bed, in which the mixture of LPG and

the air combusted, was fitted with a sample of polymer material. In the case of HDPE, after approximately 1.5 s, there was a sudden release of substantial amounts of combustible gases, whose combustion could be observed in the upper part of the reactor (Fig. 3). For most of the samples the process of combustion ran smoothly with occasional single diffusion flames. The exceptions were the materials whose monomer contained oxygen (PET, PC, PA), then the flames were observable more often. Retardation of combustion could be caused by the formation of a gas halo around the particle of the polymer, which inhibited the heat and mass conversion with the surrounding environment. The sand sticking to the sample increased its mass and solidified its structure, making the original shape of the particle visible in the bed for a long period of time. In the third second of HDPE combustion the disintegration of the agglomerate could be observed. In the final stage of the process, the gas products of decomposition or the remaining coke burnt down on the whole surface of the polymer, increasing its temperature. It was observable as a brighter area of the bed in the ninth second. The previous paper indicated a relationship between a pixel's brightness and the actual temperature of the photographed object (Żukowski et al., 2009).

In the second series of tests, just before placing the sample in the bed, the inflow of gas fuel was turned off. The fluidized bed was only a constant stream of air and its temperature decreased while taking measurements. The analysis of the recorded images of combustion led to the distinction of three periods of polymers' thermal decomposition: Induction, Flame combustion and Burnout (Fig. 4). The maxima of the brightness curve corresponded to subsequent ignitions of gas products. In the first period, when the sample was heated by the bed, the ignitions of the released gases were not observed (lack of light effects). In the case of biomass, there was a strong correlation ($R^2 = 0.98$) between the ignition temperature (Table 1) and the induction time. Such correlation did not occur in the combustion of polymers. In the second stage, the released gases combusted immediately as a result of a sudden depolymerisation. In the initial part of this stage (Figs. 4, 4315–4330 s) the volume of the combusted gases was considerably greater than in the second one – the brightness of the flares was the greatest but declined in time (Figs. 4, 4330–4340 s) which can be easily seen in the subsequent photographs of Fig. 4. In the final stage of the sample combustion, the period of burnout can be distinguished. It is the time from the termination of the flame combustion to the total decomposition of the sample in the bed.

The combustible gases released from the interior of the decomposing polymer particle flew constantly to its surface and after mixing with the air they ignited. The ignition time was determined by the composition and temperature of the gas mixture filling the bubble. When the mixture of gas fuel and oxidiser was not combustible or its temperature was too low, its ignition induction time was longer than the time the bubble remained in the bed. The ignition then occurred above the bed. The flame was propagated by the gas coming from the decreasing gaseous ring of the particle, at the same time that ring performed the function of the particle's thermal insulation. After depletion of the gas fuel emitted

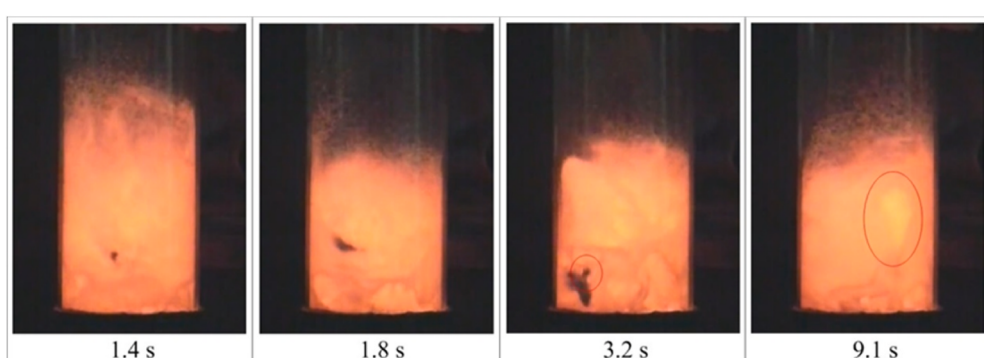


Fig. 3. Behaviour of HDPE particle (0.625 ± 0.001 g) during co-combustion. The time under the frame identifies the moment when a particular photo is taken.

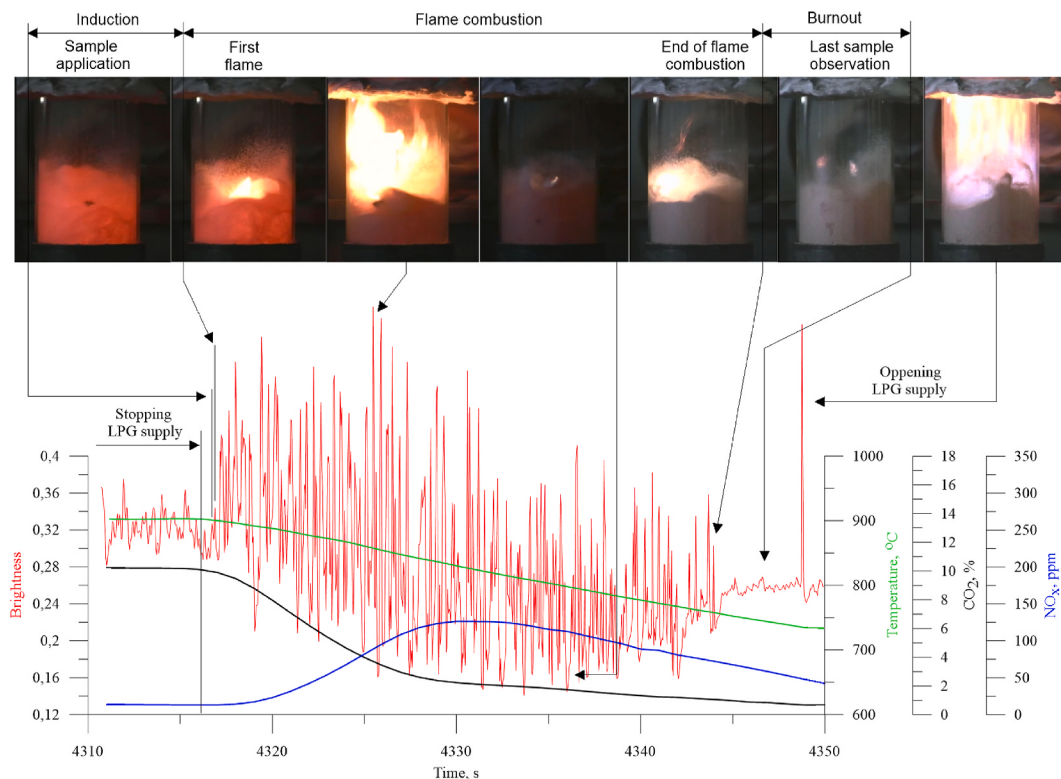


Fig. 4. Dynamics of light effects accompanying the ABS combustion.

from the polymer particle the flame faded away and the whole cycle could be repeated. The described processes of combustion of volatile parts separated from single particles of polymer polymers were stochastic. This leads to the conclusion that the dynamics of polymer material combustion in the bed might be the dynamics of a chaotic process.

The generalized diagram of the sequential phenomena that make up the dynamics of the chaotic combustion of polymers presented in Fig. 5 was based on observations and measurements that accompanied combustion. In this diagram, taking into account the recorded and measured change in brightness of the zone covering the bed and the space above the bed was taken into account while conducting the experiment. In this figure the orange ring, with a cross-section that grows or diminishes in time, represents a mixture of gas products of pyrolysis and air, before

and after its ignition. The appearance of the flame is accompanied by the value rise on the brightness curve and respective increase in the size of the heat and exhaust gases stream. The ignition of the fuel-oxidiser mixture takes place in the bed after gaining the appropriate composition and temperature, at a random time for different volumes of the mixture. Hence, the brightness curve showed lower and higher peaks. The sample dimensions, which during the process diminished together with its mass, had an impact on the speed of combustion (Baron et al., 2006).

Combustible gases mixed with air ignited irrespective of the position/location of the polymer particle in the bed. For instance, in one of the experiments (Fig. 6) in the 25th second after applying the PET sample of 1.780 ± 0.001 g into the bed, the gas bubble surrounding the

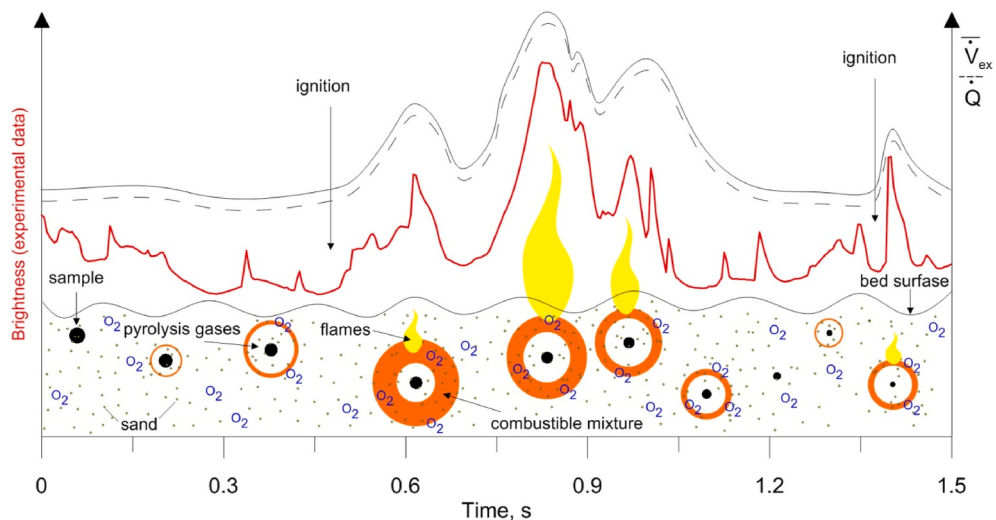


Fig. 5. Chaotic dynamics of combustion of polymer particle. \bar{V}_{ex} – stream of exhaust gases, \dot{Q} – stream of heat.

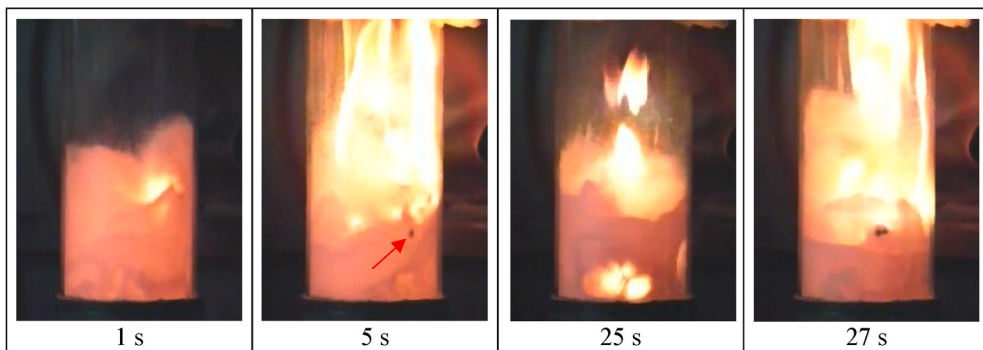


Fig. 6. Behaviour of the PET particle (1.780 ± 0.001 g) during combustion. The time under the frame identifies the moment when a particular photo is taken.

polymer particle, which was near the distributor, ignited. The sample was further amounted to the surface of the bed (27.000 ± 0.002 s). In case of PVC samples, the volume of released, combustible gases was noticeably smaller and after mixing with the oxygen they all combusted in the bed (Fig. 7). When the sample was located closer to the surface of the bed, the gas products of pyrolysis did not form mixtures in the right proportions with the air and they combusted in the diffusion flame only above the surface of the bed (Fig. 7, Picture 2).

Unlike with polymers, during the co-combustion of biomass with LPG, there was no observable sudden release of large volumes of combustible gases in the first stage of the process (Fig. 8, Picture A). The co-combustion of biomasses was accompanied by numerous diffusion flames, related to the porous structure of the cellulose which facilitated the gas penetration, and the presence of oxygen in its particle. Based on the data from the elemental CHN analysis of the combusted materials, the percentage of oxygen in the samples was determined. Elementary analysis indicated about $45 \pm 1\%$ of O₂ in the biomasses, $34 \pm 1\%$ in PET, $19 \pm 1\%$ in PC and $10 \pm 1\%$ in PA. In the case of biomasses, the pulsing character of the flame combustion was less visible, and the diffusion combustion was observed near the surface of the particle (Fig. 8, Picture B). During the combustion of the sample without additional gaseous fuel, fragments of particles split up and while finally combusting in the bed they were visible in the form of brighter points around the sample (Fig. 8, Picture B).

4.2. Co-combustion of polymers and biomass with gas fuel

Times of co-combustion of the polymers and biomass samples with gas fuel were determined on the basis of the alterations in the concentration of CO₂. With respect to materials which were combusted with diffusion flames above the bed, the duration of the flame combustion was determined by the brightness curves of single frames on the

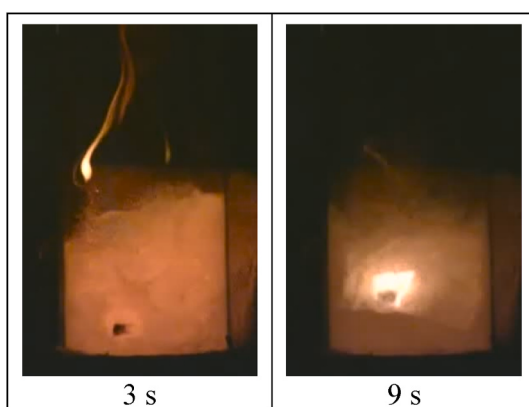


Fig. 7. Behaviour of the PVC particle (0.412 ± 0.001 g) The time under the frame identifies the moment when a particular photo is taken.

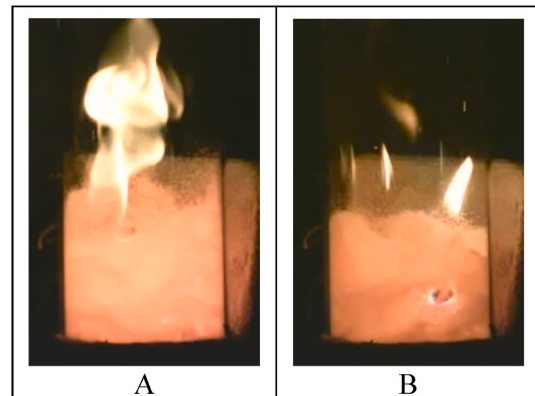


Fig. 8. Behaviour of the pine wood (0.545 ± 0.001 g and 0.410 ± 0.001 g) during co-combustion (A) and combustion (B).

recorded film (Fig. 4).

Irrespective of the samples mass, the combustion times for various packaging materials oscillated around 10.8 s (Fig. 9) in the majority of cases. Also, the time required for the construction of the polymers' decomposition was similar to that of packaging materials. The two exceptions are PVC and PA, which combusted in approximately twice as long a time. The extended combustion time for PVC could be caused by a film of char appearing on its surface. After PA combustion, the bed was covered with a porous structure made of fibreglass, which could substantially influence the polymer degassing. Co-combustion of PC, ABS and PA was conducted in the temperature of approximately $900 \pm 1^\circ\text{C}$, with $5.0 \pm 0.2\%$ vol of oxygen and of PVC in $950 \pm 1^\circ\text{C}$ with $7.0 \pm 0.2\%$ vol of oxygen. Positive correlation between combustion time and sample weight was found only in the case of PVC and ABS. Lack of correlation between combustion time and sample mass was caused by a large area of sample with respect to its volume (Baron et al., 2006). This particularly applies to samples of greater mass. Except for LDPE, which was in the form of granules, the regrinds were the research material. Greater area of the sample with small thickness (approximately 1.5 mm), encourages intensive heat exchange and increases the zone of interphase contact for a decomposition reaction. The sample consisting of a greater number of polymer particles with the largest general mass combusted in a time that was shorter than or comparable to that of smaller mass samples. The influence of the first sample's diameter on its combustion time was already observed not only in the case of polymers (Baron et al., 2006) but also for paraffin (Menon et al., 2017). Only the HDPE (Fig. 3) was defragmented in the bed. The data for Fig. 9 are collected in Table 2.

The time of biomass co-combustion with gas fuel was specified by means of two methods – the analysis of brightness changes in the zone of the bed (Fig. 10) and the magnitude of CO₂ emission (Fig. 11). Fig. 10 shows how time is measured based on the brightness curves. The

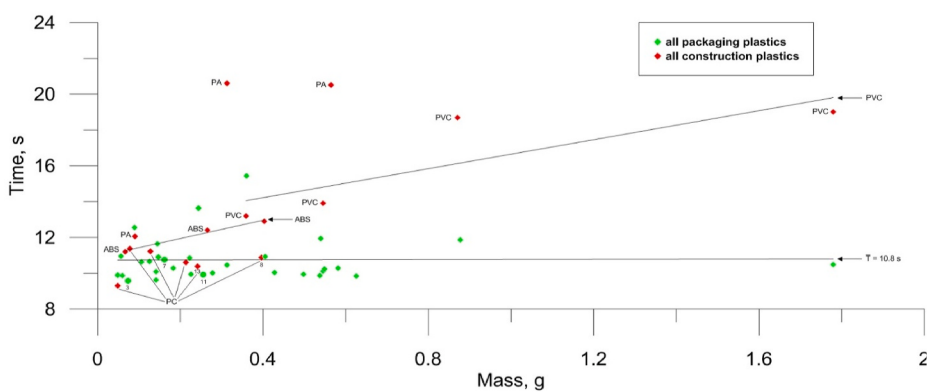


Fig. 9. Dynamics of co-combustion of LPG polymers determined by CO_2 emissions. T – average combustion time for packaging materials, \diamond - grinding, \circ – regrind, 3, 7, 8, 11, 13 - number of particles in the sample.

Table 2

Time of co-combustion of LPG polymers determined by CO_2 emissions.

Polymer	number of particles	Average particle mass, $\pm 1 \text{ mg}$	Average combustion time (from CO_2), $\pm 1 \text{ s}$
Packaging plastics			
LDPE	3	24	10
	7	23	11
	11	23	10
HDPE	1	56	11
	1	141	10
	1	222	11
	1	498	10
	1	582	10
	1	625	10
PP	1	89	13
	1	144	12
	1	36	15
	1	141	10
	1	226	10
	1	278	10
	1	405	11
	1	537	10
PS	1	48	10
	1	147	11
	1	244	14
	1	106	11
	1	183	10
	1	428	10
	1	545	10
PET	1	125	11
	7	45	11
	4	135	12
	1	549	10
	1	877	12
	1	1780	10
Construction plastics			
PC	1	128	11
	1	213	11
	8	49	11
	1	48	9
	1	78	11
PA	1	313	21
	1	564	21
ABS	1	67	11
	1	265	12
	1	403	13
PVC	1	142	22
	1	359	13
	1	545	14
	1	871	19
	1	1780	19

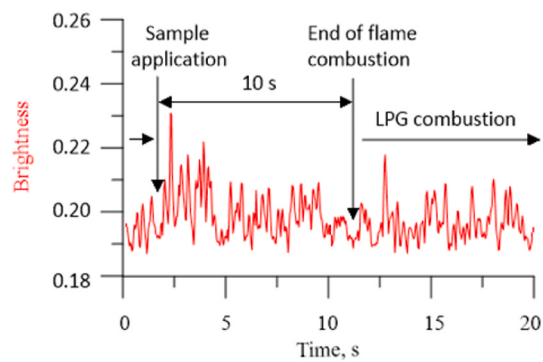


Fig. 10. Measurement of biomass co-combustion time with LPG based on brightness.

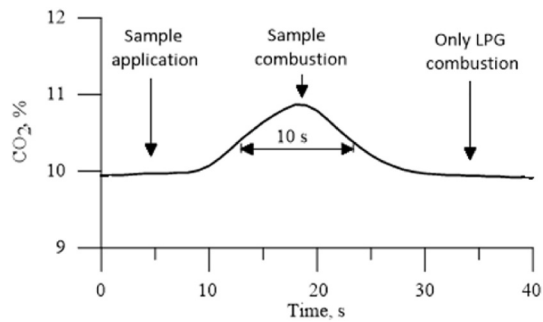


Fig. 11. Measurement of biomass co-combustion time based on CO_2 emissions.

moment of sample application to the bed and the last flames that accompanied the co-combustion with LPG were determined on the basis of image analysis. In the case of the second method, the method of measuring the time of biomass co-combustion with additional fuel is shown in Fig. 11. The co-combustion time was measured at the half of the peak height, corresponding to the change in CO_2 concentration after the sample was introduced into the bed.

In the case of biomass, it was possible to determine the co-combustion time on the basis of changes in image brightness, because numerous diffusion flames were observed during this process. Regular ignitions of flammable gases were not noticeable during the co-combustion of polymers, with exceptions such as PVC. Graph 10 shows the measured times of biomass and PVC co-combustion with LPG, based on the brightness curves, depending on the mass of the sample. The experimental data were estimated using the least squares method and the confidence intervals of this method were determined with

Nevman curves. Graph 11 shows the results for the same samples in a similar way, with the difference that the time of their co-combustion with LPG was determined based on the change in CO₂ concentration.

The results obtained by means of the first method were characterised by greater dispersion (standard deviation) SD = 15.3, better fitting of a linear regression model Standard Error of the Estimate SEE = 5.9, Mean Squared Error MSE = 35 and positive correlation R² = 0.86 (Fig. 12). With respect to the second method, the results were less scattered around the average SD = 9.8, but more around the mass of the sample SEE = 6.5, MSE = 42 with positive correlation R² = 0.58 (Fig. 13). Statistically the difference between SEE for two linear regression models was irrelevant (The value of Student test: t = 0.199, Degrees of freedom for t: df = 19, Probability of testing: p = 0.844, The critical value of Student test t_{0.05,19} = 2.093). In both cases there was a visible linear correlation between the combustion time and the sample mass, the r-Pearson coefficients essentially diverged from zero (t = 10.411 and t = 4.990, df = 18, p < 0.001, t_{0.05,18} = 2.101). The differences between slope factors of simple linear regressions at the level of trust 0.05 were statistically irrelevant (t = 1.178, df = 18, p = 0.257, t_{0.05,18} = 2.101). The average uncertainties of estimating the combustion time in both methods with 95% confidence intervals were 3.8 s and 4.2 s (Figs. 12 and 13). However, maximum values were obtained for samples with the greatest mass and they constituted 5.8 s and 6.3 s, respectively.

As opposed to polymers (Fig. 9), the combustion time for LPG depended severely on the sample mass rather than on its type, which was of less importance. Material processed in the form of briquettes and pellets (T = 28.0 ± 3.8 s) combusted in a time similar to that of wood (T = 29.0 ± 3.8 s) (Figs. 12 and 13). In comparison to polymers, the biomasses combusted longer, except for the lightest samples, whose decomposition time was close to that of packaging polymers (T = 12.1 ± 4.4 s for the samples whose average mass was m = 0.140 g). The flaming combustion time rose along with the increased sample mass and depended on its type but to a small degree. It indicates that the biomass has a similar mechanism for the combustible gases release for all its types. The dependence of flaming combustion time on the sample mass occurred only in case of PVC (T = 19.7 s), which is a bit shorter in comparison to the time required for the decomposition of the biomass samples, whose masses were similar (Fig. 12).

4.3. Combustion of polymers and biomass without gaseous fuel

Combustion of polymers and biomass in the fluidized bed without gasous fuel enabled the differentiation of characteristic stages in this

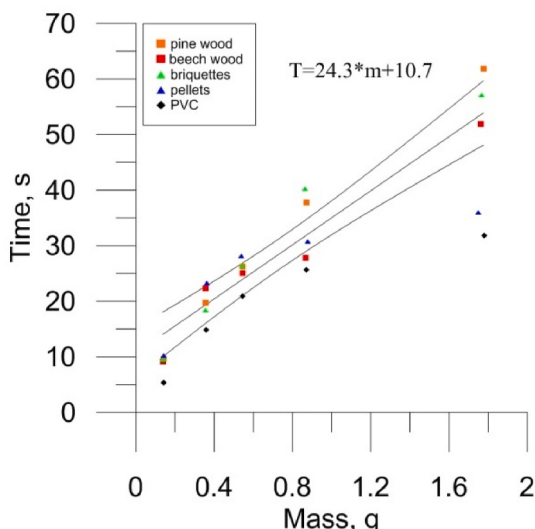


Fig. 12. Dynamics of co-combustion of the biomass and PVC with LPG (according to the brightness curve). T-time, m-mass.

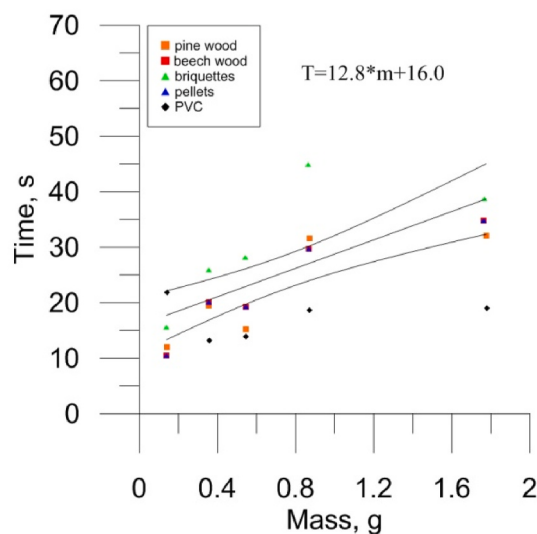


Fig. 13. Dynamics of biomass co-combustion with LPG (with respect to CO₂ emission). T-time, m-mass.

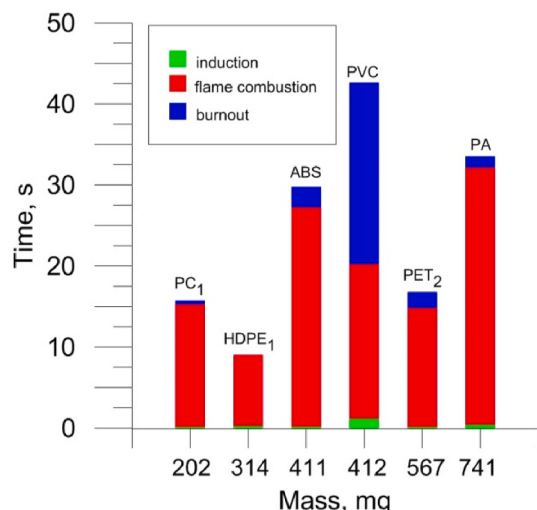


Fig. 14. Dynamics of polymers combustion without LPG with marked stages.

process and the calculation of their times (Fig. 14). The dominating stage for the majority of packaging and construction materials was the flame combustion (85.4%), with the exception of PVC (44.8%), when the sample resided in the bed for a longer period of time and did not generate any light effects. The induction time for this material was also the longest (2.6%) in comparison to the other polymers (1.2%).

Elementary analysis of the PVC utilised in the experiment indicated less content of carbon by approximately 25% in relation to the pure polymer. The number of additives can reach 70% of the polymer's mass. It suggests the presence of additional incombustible substances, for instance, flame retardants, aggregates and stabilizers which have an impact on the process of thermal decomposition of polymers. The PVC dehydrochlorination stabilisers constitute the derivatives of tin compounds like lead, zinc, and cadmium (Markarian, 2007).

The HDPE sample, which decomposed the fastest, underwent the pyrolysis in total with the emitted gases, which combusted in the diffusion flame. Combustion times for polymers combusted without the gaseous LPG were longer than those with gas fuel (Fig. 14). HDPE samples were the exception because their combustion time was not influenced by simultaneous LPG combustion. It could be caused by the fact that the polymer particle combusted before the temperature of the

bed along with the speed of the radical reactions declined substantially. Moreover, the ignition temperature PE is the lowest in comparison to other materials (Table 1). Polyolefins decompose according to a mechanism in which the bonds of the carbon chain break/crack in random place (if all bonds are energetically equivalent) resulting in the creation of monomers and oligomers. The characteristic feature of this mechanism is the formation of free radicals which maintain the process of combustion. The presence of radicals (H^* , OH^* , HO_2^* and CH_i^*) from the combustion of LPG fosters the process of further carbon chain fragmentation reducing the general time of polymers' combustion.

Opposite to polymers, the combustion of biomasses had a different division into particular stages and was dominated by flameless combustion (72.9%) (Fig. 15). The induction time for all the samples of biomass was about 0.42 s (0.4%) ($SEE = 4.3 \cdot 10^{-2}$, $MSE = 1.8 \cdot 10^{-3}$) whereas the flame combustion time was 32.95 s (26.7%) ($SEE = 2.6$, $MSE = 6.9$). It points to a similar mechanism of biomass decomposition, irrespective of its type and processing method.

The essential difference in the way polymers and biomasses combusted were the intervals between ignitions of combustible gases. The brightness curves were averaged by means of the moving average model ($k = 29$) in order to restrain temporary disturbances, and also the time between the extreme values obtained was also measured (Fig. 16). The combustion of HDPE and beech wood was conducted without LPG and with the temperature drop of about 55°C in 10 s. During this time the HDPE sample was combusted, and the temperature of the bed altered within the range of 904–852°C. The temperature of the bed during the combustion of the beech wood changed between 920 and 863°C after 10 s and declined to 524°C after 120 s when the sample burnt out. High speed of the HDPE decomposition and large amounts of the released gases caused a significant increase in the average brightness change above the brightness of the working bed (the beginning and the end of HDPE curve, Fig. 16). The combustion of the beech wood was accompanied by the release of fewer combustible gases and at a slower pace. As a result, the average value of the brightness change became close to the average of the background (Fig. 16).

Time intervals between subsequent ignitions of combustible gases during the polymers combustion were about 0.52 ± 0.06 s (2 Hz), irrespective of the mass and sample type (Fig. 17). The only exception is PVC whose value was about 0.36 ± 0.08 s (2.8 Hz), which is astonishing as it is difficult to combust (flame retardants, stabilisers, aggregates etc.). On the one hand, chlorine compounds impede the fuel combustion and extend the decomposition time but on the other hand, they act like a catalyst and accelerate the process of pyrolysis. Furthermore, the alterations in temperature, consistency, viscosity, and porosity of the sample influence the speed that the HCl bubbles transport to the gaseous phase. All these aspects may cause changes in the PVC decomposition

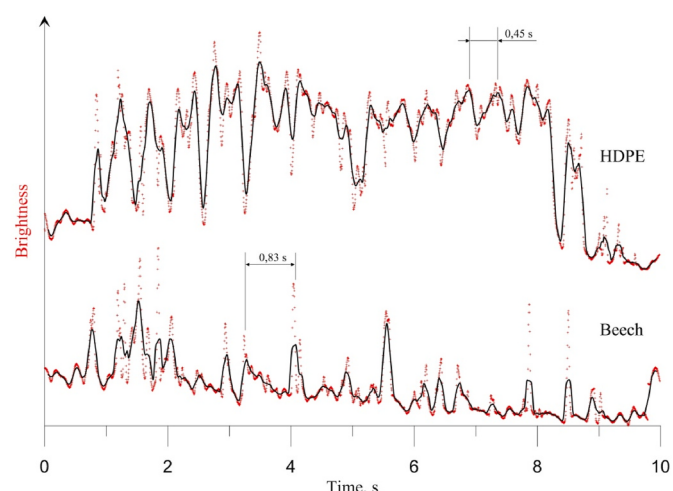


Fig. 16. Averaged dynamics of light effects during the combustion of HDPE and beech wood (without LPG).

mechanism (German, 2009). During the combustion of the biomasses the intervals between the following ignitions of combustible gases were twice as long as in the case of the polymers. Their average value was about 0.90 ± 0.08 s (1.1 Hz). The difference in the rate of release and flame combustion of combustible gases may result from various mechanisms of decomposition of biomasses and polymers.

5. Conclusion

The aim of the study was to describe the characteristic phenomena that accompany the combustion of polymers, which affect the dynamics of the combustion process and their thermal transformation. This goal was achieved by showing the phenomena occurring in the fluidized bed during combustion of polymers, and the combustion times of various materials were measured and compared. For comparative purposes, analogous tests were carried out for the biomasses.

The combustion of materials containing polymer links in the fluidized bed, such as polymers and biomasses, took place in various ways. Polymers melted and combined with sand in high temperatures, which led to changes in their density and surface structure. It was accompanied by a sudden release of large volumes of pyrolytic gases whose ignition after mixing with oxidiser occurred with a frequency of about 2 Hz. The exception was PVC, in which case there were more frequent ignitions of combustible gases – around 2.8 Hz. The tests confirmed the influence of the polymers initial dimensions on their combustion time – shredded samples with smaller diameters combusted faster (Fig. 9). The biomasses combusted slower and released less volumes of combustible gases with an ignition frequency of about 1.1 Hz.

Combustion times of packaging and construction materials were close to each other ($T = 10.8$ s), except for PVC and PA, whose combustion times were twice as long. The layer of char, formed as a result of netting non-volatile products of pyrolysis, which stops the diffusion of oxygen and transfer of heat into the sample and is, among others, responsible for the extension of the polymers' combustion time. The time of combustion of LPG biomasses, as opposed to polymers, depended severely on the mass of the sample and to a small extent on its type – briquettes and pellets ($T = 28.0 \pm 3.8$ s) combusted in time approximate to the combustion of wood ($T = 29.0 \pm 3.8$ s). The biomasses had a longer combustion time than polymers, except for the lightest samples ($m = 0.140$ g) whose combustion time was close to that of packaging materials ($T = 12.1 \pm 4.4$ s). The presence of radicals coming from the combustion of LPG as well as a homogeneous temperature field of the fluidized bed fostered the process of further fragmentation of the carbon chain, shortening the general combustion time of polymers in

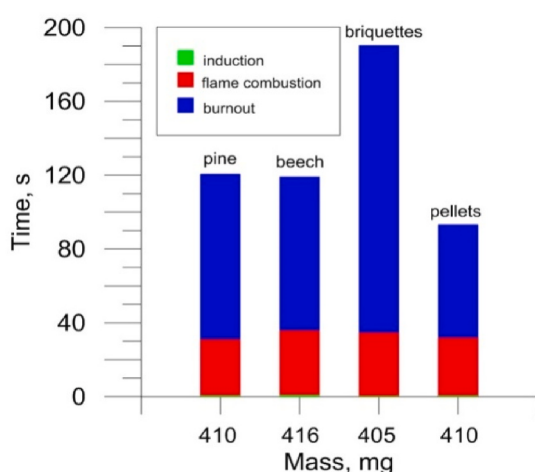


Fig. 15. Dynamics of biomass combustion without LPG with marked stages.

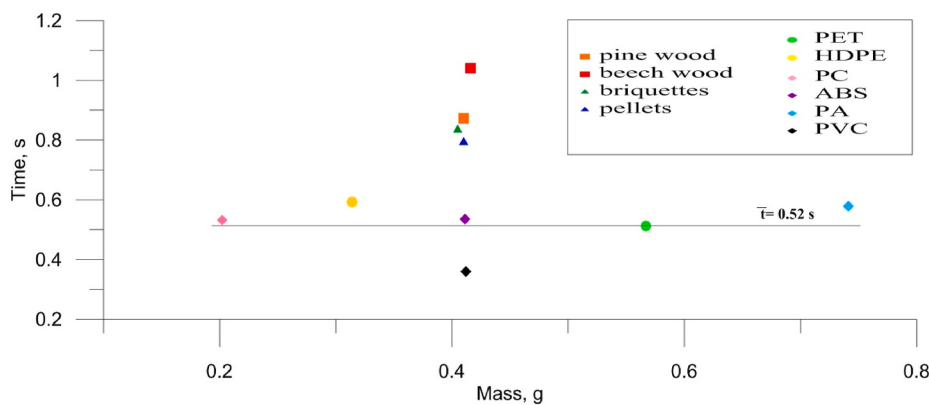


Fig. 17. Average times between ignitions of combustible gases inside the bed. \bar{t} -average time for polymers.

comparison to tests without the gaseous LPG. The dominating stage during the combustion of polymers was the flame combustion, which constituted 85.4% of the whole time required for the combustion of the sample. The biomass was the opposite case, where the flameless combustion constituted 72.9%, the flame combustion was 26.7% of the needed time. The induction time of polymers in the bed was 1.2%, including 2.6% of PVC. The differences in the behaviour of the particles in the fluidized bed, the rate of releasing the combustible gases and their flame combustion may be caused by the various decomposition mechanisms of biomasses and polymers.

CRediT authorship contribution statement

Witold Źukowski: Conceptualization, Methodology, Investigation, Supervision, Writing – review & editing. **Dawid Jankowski:** Resources, Formal analysis, Investigation, Visualization, Writing – original draft. **Jerzy Baron:** Resources, Investigation, Writing – original draft. **Jan Wrona:** Investigation, Resources, Validation, Visualization, Writing – review & editing.

Declaration of competing interest

The authors declare that they have no known competing financial interests or personal relationships that could have appeared to influence the work reported in this paper.

References

- Akram, M., Tan, C.K., Garwood, R., Thai, S.M., 2015. Vinasse – a potential biofuel – cofiring with coal in a fluidised bed Combustor. *Fuel* 158, 1006–1015.
- Al-Salem, S.M., Antelava, A., Constantinou, A., Manos, G., Dutta, A., 2017. A review on thermal and catalytic pyrolysis of plastic solid waste (PSW). *J. Environ. Manag.* 197, 177–198.
- Baron, J., Bulewicz, E.M., Kandefer, S., Pilawska, M., Źukowski, W., Hayhurst, A.N., 2006. The combustion of polymer pellets in a bubbling fluidised bed. *Fuel* 85, 2494–2508.
- Baytekin, B., Baytekin, H.T., Grzybowski, B.A., 2013. Retrieving and converting energy from polymers: deployable technologies and emerging concepts. *Energy Environ. Sci.* 6 (12), 3467–3482.
- Berkowicz, G., Majka, T.M., Źukowski, W., 2020. The pyrolysis and combustion of polyoxymethylene in a fluidised bed with the possibility of incorporating CO₂. *Energy Convers. Manag.* 214, 112888.
- Berkowicz, G., Źukowski, W., Baron, J., 2013. Effect of temperature on o-cresol methylation in a fluidized bed of commercial iron-chromium catalyst TZC-3/1. *Pol. J. Chem. Technol.* 15 (3), 100–102.
- Boryniec, S., Przygocki, W., 2000. Polymer combustion processes. Part I. Fundamental problems. *Prog. Rubber Plast. Technol.* 16 (3), 193–210.
- Boryniec, S., Przygocki, W., 1999. Combustion of polymers. Part III. Fire retardants for polymeric materials. *Polymers* 44 (10), 656–665.
- Burgess, F., Lloyd, P.D.W., Fennell, P.S., Hayhurst, A.N., 2011. Combustion of polymer pellets in a bubbling fluidised bed. *Combust. Flame* 158 (8), 1638–1645.
- Chen, Y., Jensen, I.G., Kirkerud, J.G., Bolkesjø, T.F., 2021. Impact of fossil-free decentralized heating on northern European renewable energy deployment and the power system. *Energy* 219, 119576.
- Chern, J.-S., Hayhurst, A.N., 2012. Fluidised bed studies of: (i) Reaction-fronts inside a coal particle during its pyrolysis or devolatilisation, (ii) the combustion of carbon in various coal chars. *Combust. Flame* 159, 367–375.
- Chern, J.-S., Hayhurst, A.N., 2010. A simple theoretical analysis of the pyrolysis of an isothermal particle of coal. *Combust. Flame* 157 (5), 925–933.
- Costiuc, L., Tieean, M., Baltes, L., Patachia, S., 2015. Experimental investigation on the heat of combustion for solid plastic waste mixtures. *Environ. Eng. Manag. J.* 14 (6), 1295–1302.
- Dong, J., Tang, Y., Nzhou, A., Chi, Y., Weiss-Hortala, E., Ni, M., Zhou, Z., 2018. Comparison of waste-to-energy technologies of gasification and incineration using life cycle assessment: case studies in Finland, France and China. *J. Clean. Prod.* 203, 287–300.
- Dwivedi, P., Mishra, P.K., Mondal, M.K., Srivastava, N., 2019. Non-biodegradable polymeric waste pyrolysis for energy recovery. *Helijon* 5, e02198.
- Ergut, A., Levendis, Y.A., Carlson, J., 2007. Emissions from the combustion of polystyrene, styrene and ethylbenzene under diverse conditions. *Fuel* 86, 1789–1799.
- European Parliament, 2018a. Directive 2018/2001/EC on the promotion of the use of energy from renewable sources. <https://eur-lex.europa.eu/legal-content/EN/TXT/?uri=CELEX:32018L2001&qid=1613661156096>.
- European Parliament, 2018b. Directive 2018/410/EC of amending Directive 2003/87/EC to enhance cost-effective emission reductions and low-carbon investments, and Decision (EU) 2015/1814. <https://eur-lex.europa.eu/legal-content/EN/TXT/PDF/?uri=CELEX:32018L0410&qid=1613661156096&from=PL>.
- Faravelli, T., Bozzano, G., Colombo, M., Ranzi, E., Dente, M., 2003. Kinetic modeling of the Thermal degradation of polyethylene and polystyrene mixtures. *J. Anal. Appl. Pyrolysis* 70, 761–777.
- Finney, K.N., Sharifi, V.N., Swithenbank, J., 2009. Combustion of spent mushroom compost and coal tailing pellets in a fluidised-bed. *Renew. Energy* 34, 860–868.
- German, K., 2009. Selected Aspects of Waste Recycling of Poly(vinyl Chloride). Monograph 372. Cracow University of Technology, Poland.
- Gomez-Campos, A., Vialle, C., Rouilly, A., Hamelin, L., Rogeon, A., Hardy, D., Sablayrolles, C., 2021. Natural Fibre Polymer Composites - a game changer for the aviation sector? *J. Clever Prod.* 286, 124986.
- Grand, A.F., Wilkie, C.H.A., 2000. Fire Retardancy of Polymeric Materials. Marcel Dekker Inc, New York.
- Hayhurst, A.N., 2013. The kinetics of the pyrolysis or devolatilization of sewage sludge and other solid fuels. *Combust. Flame* 160, 138–144.
- Horvath, J., Balog, K., 2013. Ignition temperature of dust layer and dust clouds of wood pellets. Research Papers Faculty of Materials Science and Technology in Trnava. Slovak University of Technology in Bratislava, pp. 122–126.
- IEA, 2018. Explore energy data by category, indicator, country or region. <https://www.iea.org/data-and-statistics/data-tables/?country=WORLD&energy=Electricity&year=2018>.
- IEA, 2017. IRENA. Perspectives for the Energy Transition. OECD/IEA and IRENA. https://www.irena.org/-/media/Files/IRENA/Agency/Publication/2017/Mar/Perspectives_for_the_Energy_Transition_2017.pdf.
- Jordan, K.J., Stib, S.L., Koberstein, J.T., 2001. Determination of the degradation mechanism from the kinetic parameters of dehydrochlorinated poly(vinyl chloride) decomposition. *J. Phys. Chem. B* 105, 3174–3181.
- Kaewbuddee, Ch., Sukjit, E., Srisertpol, J., Maithomklang, S., Wathakit, K., Klinkaew, N., Liplap, P., Arjharn, W., 2020. Evaluation of waste plastic oil-biodiesel blends as alternative fuels for diesel engines. *Energies* 13, 2823.
- Kasara, P., Sharma, D.K., Ahmaruzzaman, M., 2020. Thermal and catalytic decomposition of waste plastics and its co-processing with petroleum residue through pyrolysis process. *J. Clean. Prod.* 265, 121639.
- Kosajan, V., Wena, Z., Fei, F., Dingaa, Ch.D., Wang, Z., Zhan, J., 2020. The feasibility analysis of cement kiln as an MSW treatment infrastructure: from a life cycle environmental impact per specific. *J. Clean. Prod.* 267, 122113.
- La Rosa, A.D., Recca, G., Summerscales, J., Latteri, A., Cozzo, G., Cicala, G., 2014. Bio-based versus traditional polymer composites. A life cycle assessment perspective. *J. Clean. Prod.* 74, 135–144.

- Liu, Q., Zhong, W., Tang, R., Yu, H., Gu, J., Zhou, G., Yu, A., 2021. Experimental tests on co-firing coal and biomass waste fuels in a fluidised bed under oxy-fuel combustion. *Fuel* 28615, 119312.
- López, A., de Marco, I., Caballero, B.M., Laresgoiti, M.F., Adrados, A., 2011. Dechlorination of fuels in pyrolysis of PVC containing plastic wastes. *Fuel Process. Technol.* 92, 253–260.
- Marczak, D., Lejcū, K., Misiewicz, J., 2020. Characteristics of biodegradable textiles used in environmental engineering: a comprehensive review. *J. Clean. Prod.* 268, 122129.
- Mark, J.E., 2007. Physical Properties of Polymers Handbook. Springer Verlag, New York.
- Markarian, J., 2007. PVC additives – what lies ahead? *Plastics, Addit. Compd.* 9, 22–25.
- Malav, L.C., Yadav, K.K., Gupta, N., Kumar, S., Sharmad, G.S., Krishnan, S., Rezania, S., Kamyab, H., Pham, Q.B., Yadav, S., Bhattacharyya, S., Yadav, V.K., Bach, Q.-V., 2020. A review on municipal solid waste as a renewable source for waste-to-energy project in India: current practices, challenges, and future opportunities. *J. Clean. Prod.* 277, 123227.
- Mazzoni, L., Janajreh, I., 2017. Plasma gasification of municipal solid waste with variable content of plastic solid waste for enhanced energy recovery. *Int. J. Hydrogen Energy* 42 (30), 19446–19457.
- McGauran, T., Dunne, N., Smyth, B.M., Cunningham, E., 2021. Feasibility of the use of poultry waste as polymer additives and implications for energy, cost and carbon. *J. Clean. Prod.* 291, 125948.
- Menon, A., Waller, N., Wenting, H., Hayhurst, A.N., Davidson, J.F., Scott, S.A., 2017. The combustion of solid paraffin wax and liquid glycerol in a fluidised bed. *Fuel* 199, 447–455.
- Moreno-Maroto, J.M., Gonzalez-Corrochano, B., Alonso-Azcarate, J., Garcia, C.M., 2019. A study on the valorization of a metallic ore mining tailing and its combination with polymeric wastes for lightweight aggregates production. *J. Clean. Prod.* 212, 997–1007.
- Nordin, A., Strandberg, A., Elbasher, S., Åmand, L.E., Skoglund, N., Pettersson, A., 2020. Co-combustion of municipal sewage sludge and biomass in a grate fired boiler for phosphorus recovery in bottom ash. *Energies* 13, 1708.
- Ortiz, P.S., Florez-Orrego, D., Oliveira Jr., S., Filho, R.M., Osseweijer, P., Posada, J., 2020. Unit exergy cost and specific CO₂ emissions of the electricity generation in The Netherlands. *Energy* 208, 118279.
- Papadis, E., Tsatsaronis, G., 2020. Challenges in the decarbonization of the energy sector. *Energy* 205, 118025.
- Patel, K., Velazquez, A., Calderon, H.S., Brown, G.R., 1992. Studies of the solid-state thermal degradation of PVC. I. Autocatalysis by hydrogen chloride. *J. Appl. Polym. Sci.* 46 (1), 179–187.
- Patel, H., Manguliya, H., Maiti, P., Maiti, S., 2021. Empty cotton boll crop-residue and plastic waste valorization to bio-oil, potassic fertilizer and activated carbon – a bio-refinery model. *J. Clean. Prod.* 290, 125738.
- Pike, R.D., Starnes Jr., W.H., Jeng, J.P., Bryant, W.S., Kourtesis, P., Adams, C.W., Bunge, S.D., Kang, Y.M., Kim, A.S., Kim, J.H., Macko, J.A., O'Brien, C.P., 1997. Low-valent metals as reductive cross-linking agents: a new strategy for smoke suppression of poly(vinyl chloride). *Macromolecules* 30 (22), 6957–6965.
- PlasticsEurope, 2020. An Analysis of European Plastics Production, Demand and Waste Data. <https://www.plasticseurope.org/en/resources/publications/4312-plastics-facts-2020>.
- Ranzi, E., Dentea, M., Faravellia, T., Bozzanoa, G., Fabinia, S., Navaa, R., Cozzani, V., Tognotti, L., 1997. Kinetic modeling of polyethylene and polypropylene thermal degradation. *J. Anal. Appl. Pyrolysis* 40 (41), 305–319.
- Razuan, R., Chen, Q., Finney, K.N., Russell, N.V., Shari, V.N., Swindenbank, J., 2011. Combustion of oil palm stone in a pilot-scale fluidised bed reactor. *Fuel Process. Technol.* 92 (12), 2219–2225.
- Roberts, B.C., Jones, A.R., Ezekeye, O.A., Ellison, C.J., Webber, M.E., 2017. Development of kinetic parameters for polyurethane thermal degradation modeling featuring a bioinspired catecholic flame retardant. *Combust. Flame* 177, 184–192.
- Saeed, L., Tohka, A., Haapala, M., Zevenhoven, R., 2004. Pyrolysis and combustion of PVC, PVC-wood and PVC-coal mixtures in a two-stage fluidized bed process. *Fuel Process. Technol.* 85, 1565–1583.
- Sánchez-Jiménez, P.E., Perejón, A., Criado, J.M., Diánez, M.J., Pérez-Maqueda, L.A., 2010. Kinetic model for thermal dehydrochlorination of poly(vinyl chloride). *Polymer* 51, 3998–4007.
- Scharler, R., Gruber, T., Ehrenhofer, A., Kelz, J., Bardar, R.M., Bauer, T., Hochenauer, C., Anca-Couce, A., 2020. Transient CFD simulation of wood log combustion in stoves. *Renew. Energy* 145, 651–662.
- Scheirs, J., Kaminsky, W., 2006. Feedstock Recycling and Pyrolysis of Waste Plastics: Converting Waste Plastics into Diesel and Other Fuels. John Wiley & Sons, Ltd.
- Singh, R.K., Ruj, B., 2016. Time and temperature depended fuel gas generation from pyrolysis of real world municipal plastic waste. *Fuel* 174, 164–171.
- Starnes, W.H., Ge, X., 2004. Mechanism of autocatalysis in the thermal dehydrochlorination of poly(vinyl chloride). *Macromolecules* 37, 352–359.
- Sun, Q., Shi, X., Lin, Y., Zhu, H., Wang, X., Cheng, C., Liu, J., 2007. Thermogravimetric-mass spectrometric study of the pyrolysis behavior of PVC. *J. China Univ. Min. Technol.* 17 (2), 242–245.
- Troitskii, B.B., Troitskaya, L.S., 1995. Mathematical models of the initial stage of the thermal degradation of poly(vinyl chloride)-3. The thermal degradation of poly(vinyl chloride) in the presence of HCl. *Eur. Polym. J.* 31 (6), 533–539.
- Troitskii, B.B., Troitskaya, L.S., 1999. Degenerated branching of chain in poly(vinyl chloride) thermal degradation. *Eur. Polym. J.* 35 (12), 2215–2224.
- Walters, R.N., Hackett, S.M., Lyon, R.E., 2000. Heats of combustion of high temperature polymers. *Fire Mater.* 24 (5), 245–252.
- Westblad, Ch., Levendis, Y.A., Richter, H., Howard, J.B., Carlson, J., 2002. A study on toxic organic emissions from batch combustion of styrene. *Chemosphere* 49, 395–412.
- Wienczel, P., Szlęk, A., Ditaranto, M., 2020. Waste-to-energy technology integrated with carbon capture e Challenges and opportunities. *Energy* 198, 117352.
- Williams, P.T., Williams, E.A., 1999. Interaction of plastics in mixed-plastics pyrolysis. *Energy Fuels* 13, 188–196.
- Wrona, J., 2014. An introduction to an installation for the production of alternative fuels from waste polyolefin Technical Transactions. *Environ. Eng.* 20, 65–72.
- Yasin, S., Curti, M., Rovero, G., Hussain, M., Sun, D., 2020. Spouted-bed gasification of flame retardant textiles as a potential non-conventional biomass. *Appl. Sci.* 10, 946.
- Yasin, S., Curti, M., Rovero, G., Behary, N., Perwuelz, A., Giraud, S., Migliavacca, G., Chen, G., Guan, J.-p., 2017. An alternative for the end-of-life phase of flame retardant textile products: degradation of flame retardant and preliminary settings of energy valorization by gasification. *BioResources* 12 (3), 5196–5211.
- Yu, J., Sun, L., Ma, C., Qiao, Y., Yao, H., 2016. Thermal degradation of PVC: a review. *Waste Manag.* 48, 300–314.
- Yuan, G., Chen, D., Yin, L., Wang, Z., Zhao, L., Wang, J.Y., 2014. High efficiency chlorine removal from polyvinyl chloride (PVC) pyrolysis with a gas–liquid fluidized bed reactor. *Waste Manag.* 34, 1045–1050.
- Zaini, I.N., Gomez-Rueda, Y., Lopez, ChG., Ratnasari, D.K., Helsen, L., Pretz, T., Jonsson, P.G., Yang, W., 2020. Production of H₂-rich syngas from excavated landfill waste through steam co-gasification with biochar. *Energy* 207, 118208.
- Zhang, W., Zhang, J., Ding, Y., He, Q., Lu, K., Chen, H., 2021. Pyrolysis kinetics and reaction mechanism of expandable polystyrene by multiple kinetics methods. *J. Clean. Prod.* 285, 125042.
- Zhou, L.W., Wang, R.Z., 2017. Urban biomass and methods of estimating municipal biomass resources. *Renew. Sustain. Energy Rev.* 80, 1017–1030.
- Żukowski, W., Baron, J., Bulewicz, E.M., Kowarska, B., 2009. An optical method of measuring the temperature in a fluidised bed combustor. *Combust. Flame* 156, 1445–1452.
- Żukowski, W., Berkowicz, G., 2019a. The combustion of polyolefins in inert and catalytic fluidised beds. *J. Clean. Prod.* 236, 117663.
- Żukowski, W., Berkowicz, G., 2019b. The combustion of liquids and low-density solids in a cenospheric fluidise d b e d. *Combust. Flame* 206, 476–489.
- Żukowski, W., Berkowicz, G., 2017. Hydrogen production through the partial oxidation of methanol using N₂O in a fluidised bed of an iron-chromium catalyst. *Int. J. Hydrogen Energy* 42, 28247–28253.